



**John L. Volakis**  
Rad. Lab., EECS Dept.  
University of Michigan  
Ann Arbor, MI 48109-2122  
(734) 647-1797  
(734) 647-2106 (Fax)  
volakis@umich.edu (email)

### Forward by JLV

This paper brings to our attention a useful tool for the analysis of antennas mounted on various platforms. Following the original work pioneered at the Ohio State University ElectroScience Lab, the authors also use the Uniform Geometrical Theory of Diffraction (UTD) for their analysis. Some features of the program that I found interesting are that it works on PCs with the *Windows* OS, and it

comes with a graphical interface for entering the geometry, visualizing it, and displaying the mechanisms. In addition, it allows the description of the geometry using planar or curved surfaces/patches entered in DXF format, for linking with commercial packages. Both metallic and non-metallic surfaces can be handled, of course, in the context of UTD. Also, the *z* buffer is used for speeding-up the ray-tracing calculations. Please contact the authors directly if you are interested in the package.

## ***FASANT*: Fast Computer Tool for the Analysis of On-Board Antennas**

***J. Pérez<sup>1</sup>, F. Saez de Adana<sup>1</sup>, O. Gutierrez<sup>1</sup>, I. Gonzalez<sup>1</sup>,  
M. F. Cátedra<sup>1</sup>, I. Montiel<sup>2</sup>, J. Guzmán<sup>2</sup>***

<sup>1</sup>Dept. de Teoría de la Señal y Comunicaciones  
Universidad de Alcalá

<sup>2</sup>Instituto Nacional de Técnica Aeroespacial (INTA)  
Universidad de Alcalá, Campus Universitario  
Ctra Madrid-Barcelona, Km 33,600  
28871 Alcalá de Henares (Madrid)  
Spain  
Fax: + 34 91 885 67 24  
E-mail: felipe.catedra@alcala.es

**Keywords:** Design automation software; Uniform Theory of Diffraction; marine vehicles; aircraft antennas; satellite antennas; numerical analysis

### **1. Abstract**

*FASANT* is a computer tool for the analysis of antennas on-board satellites, ships, aircraft, and other complex bodies. The structure under analysis, which can be metallic or dielectric (with and/or without losses), must be modeled by plane and/or curved surfaces. The geometrical input files are in DXF format, and can be generated by the most commonly used computer-aided geometrical-design (CAGD) tools. The code can also be applied to the analysis of arrays and arbitrarily shaped reflectors. The kernel of the code is based on the Uniform Theory of Diffraction (UTD). Special algorithms have been developed to speed up the ray-tracing

computation for both flat and curved surfaces. *FASANT* can obtain far-field patterns, field levels at points near the structure, can calculate the mutual coupling between antennas or between array elements, and can show each ray-tracing mechanism.

### **2. Functionality and methodology**

***F*** *ASANT* is an accurate and efficient tool to analyze antennas on-board complex structures. The geometrical input data are based on a three-dimensional plane-and-curved-facets model of the structure, which is given in terms of DXF files. Each facet of the model has associated with it the corresponding material and, in this way, *FASANT* can treat structures made of different materials. *FASANT* is able to read DXF files from *AUTOCAD*, *Microsystem*, *CADD*S, and other CAGD tools. In addition, *FASANT* has its own facility, which allows it to modify the geometry, or to create a new

one. *FASANT* visualizes the geometry on the computer screen as two-dimensional projections or as three-dimensional views. The user can zoom the geometry, and modify it in a graphical and iterative way.

The electromagnetic analysis is performed using UTD techniques [1]. The UTD mechanisms that can be considered are:

- Direct field
- Reflected field
- Diffracted field
- Double-reflected field
- Reflected-diffracted field
- Diffracted-reflected field
- Double-diffracted field
- Slope-diffracted field
- Vertex-diffracted field
- Double-reflected field in curves
- Reflected-diffracted field in curves
- Diffracted-reflected field in curves
- Transmitted field
- Transmitted-reflected field
- Reflected-transmitted field
- Transmitted-diffracted field
- Diffracted-transmitted field
- Near or far field due to creeping waves

Another important feature of *FASANT* is that it lets you see the *ray tracing* of each effect considered in the simulation. The program uses a friendly graphical interface, which is both quick and easy to handle. It lets you see the geometry under analysis from any point of view, situate the antenna, see the results with different options, etc.

A new ray-tracing algorithm is used to speed up the computations. This ray-tracing algorithm is based on a modification of the *z*-buffer and the "Bounding Volumes" schemes, in which the elements are arranged in an angular map (AZB, angular *z*-buffer) [2].

### 3. Language and computer on which code runs

The kernel of *FASANT* is written in *FORTRAN*. The graphics and the user interface have been developed using the *FORTRAN Powerstation* of Microsoft. The code runs on any platform with *Windows 95* or *Windows NT 4.x*. A minimum of 16 MB of RAM is required (32 MB or more recommended). The kernel can be easily made to run in any machine.

### 4. Input data

*FASANT* reads three input files: one file defining the geometry of the structure, another one defining the transmitting antenna, and the third that specifies the remaining parameters.

#### 4.1 Geometry file

The geometry is defined by a DXF file, in terms of plane polygonal facets and/or curved surfaces, modeled by polylines or NURBS (Non-Uniform Rational B-Spline) [3]. Two geometries are shown in Figures 1 and 2. *FASANT* allows us to visualize the geometry from any point, presenting (or not presenting) the hidden surfaces.

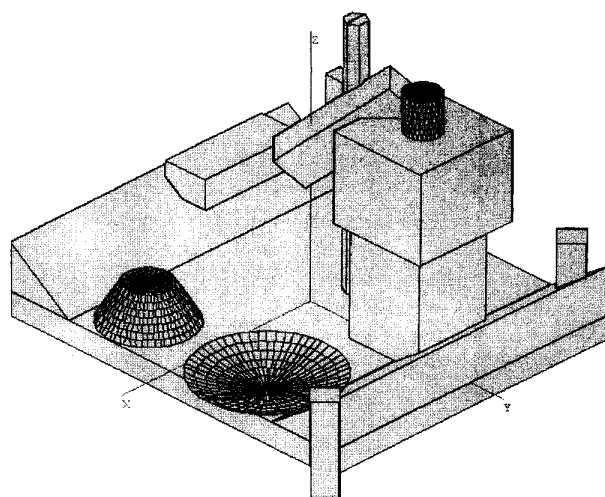


Figure 1. The geometry of the HISPASAT satellite.

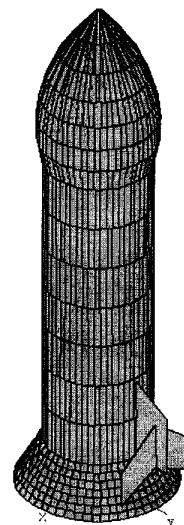


Figure 2. The geometry of a missile.

The facets or curved surfaces that form the geometry do not have to be perfect conductors, but they can be made of any other material. There is an auxiliary file that indicates the material of all the facets and curved surfaces of the model.

The geometric model can be generated by an external CAGD tool, or by *FASANT*, itself. The user can modify a previous geometry, deleting or modifying an existing facet or curved surface, or adding a new one. These options are easier with the zoom facility of *FASANT*.

#### 4.2 Radiation-pattern file

The second kind of input data for *FASANT* contains information about the radiation pattern of the antennas. This file is not always required, because the transmitter antenna can be specified as a set of infinitesimal dipoles, as shown in Section 4.3.

The radiation pattern of an antenna can have three different formats: a) symmetry of revolution; b) defined by the E plane and the H plane [4]; or c) in a full three-dimensional manner, specified by the amplitude and phase values in some directions ( $\theta, \phi$ ). For cases a) and b), the z axis is forced to be the axis of symmetry.

The radiation pattern can be given in terms of linear polarization or in circular polarization. For linear polarization, the field will be given in terms of the  $\theta$  and  $\phi$  components, while for circular polarization, the field will be in terms of  $E_{U_l}$  and  $E_{U_d}$  (left and right polarization, respectively).

#### 4.3 Parameter data

This set of input data can be easily generated using the graphical interface of *FASANT*. The following data are required:

- The simulation type to be performed. Three options are possible: FAR, NEAR, and COUPLING. The first option provides the far field in directions of observation that are indicated in the Angular Sweep Type entrance (see below). The second option obtains the Field Level at the observation points that are defined in the Observation Points entrance (see below), and the third calculates the coupling between two antennas in the presence of the structure. In the two first cases, the user can visualize a Ray Tracing File (see Section 5), which contains the ray trajectory of each effect selected.

- The ray mechanisms to be considered (direct ray, reflected ray, diffracted ray, etc.).

- The location of the transmitter antenna, the orientation of its axis, and the radiated power. The orientation of the antenna is specified by the direction cosines that associate the axis of the antenna to the absolute coordinate system. The antenna coordinate system is that wherein the antennas are described, and the absolute coordinate system is that to which the geometry, the observation points, and the results are referenced.

The transmitter antenna can be defined as a set of infinitesimal dipoles, or from a radiation-pattern file. In the first case, it is necessary to enter the number of electric and magnetic dipoles, the product between the length and the current of each dipole (amplitude and phase), and the location of coordinates and the direction

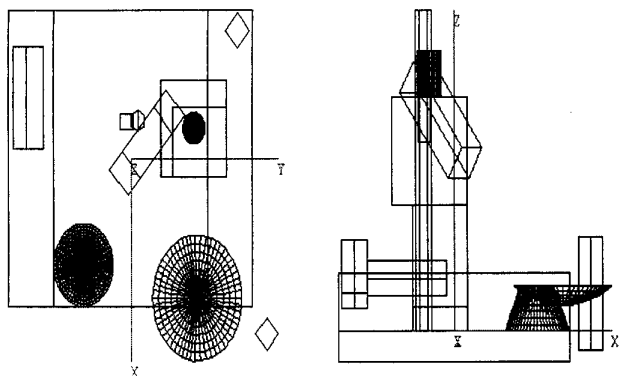


**Figure 3.** Geometrical views for the antenna location using the mouse.

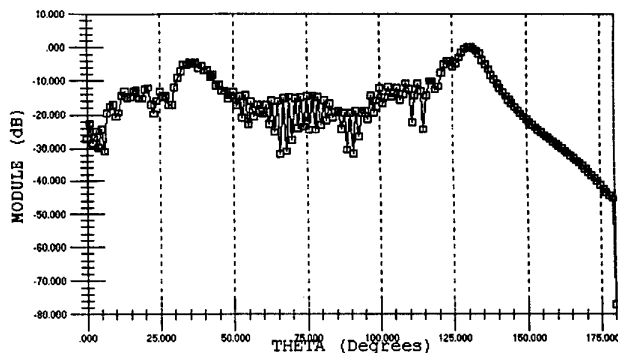


**Figure 4.** The field level output.

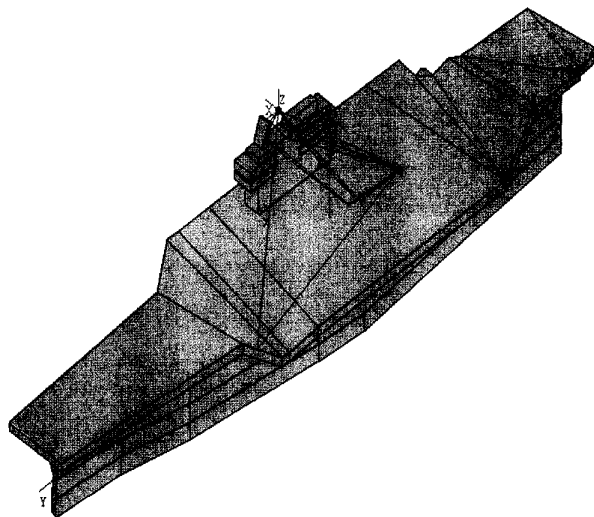


**Figure 5a.** A ray-tracing visualization.

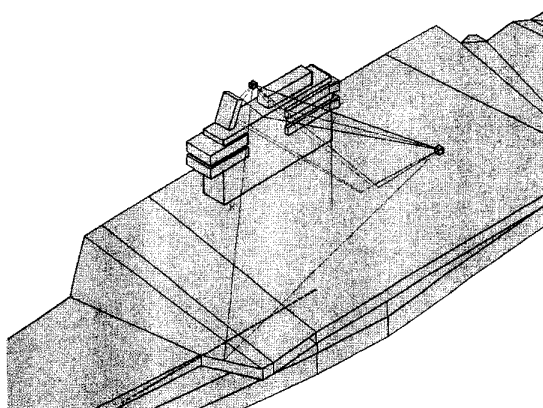


**Figure 5b.** A ray-tracing visualization using the zoom facility.

cosines associated with each dipole relative to the antenna coordinate system. Internal to *FASANT*, a local coordinate system is associated to each of the dipoles, the axes of the dipoles being parallel to the z axis of their systems. For the second case (radiation pattern defined from a file), only the name of the file, its format, and polarization must be specified. The location and orientation of the antenna can be entered through the keyboard or graphically, using a mouse.

*FASANT* allows us to simulate one of several antennas at the same time; therefore, it can allow for analysis of on-board arrays. Frequency sweeping is allowed by giving the initial and final frequencies, along with the number of computations within the specified bandwidth. Other input parameters are requested, depending on the type of simulation:

- The directions of observation for computing the far field, if the FAR option is chosen.

- The observation points for computing the field level, if the NEAR option is chosen. *FASANT* can accept these points from an external file, or by using the graphical user interface. In the latter case, the points can be selected along a straight line, or as a mesh forming a rectangle.

- The receiver-antenna data (defined in the same way indicated for the transmitter antenna), if the COUPLING option is chosen.

*FASANT* accepts the coordinates of the antenna and observation points either exactly, with the keyboard, or approximately, using the mouse. Figure 3 is an example visualization of the structure on which the user can "click," using the mouse to specify the antenna location.

## 5. Output data

The output of *FASANT* is a file containing the field levels at each direction of observation, if the FAR option is chosen, or at the observation points chosen in conjunction with the NEAR option. If the COUPLING option is chosen, the output file will contain the coupling between the transmitting and receiving antennas. In all options, it is possible to visualize the ray tracing.

### 5.1 Field levels

The results are visualized in an  $x$ - $y$  graphic, as shown in Figure 4. The  $x$  axis indicates the angle of the observation point, and the  $y$  axis corresponds to the field level, in dB.

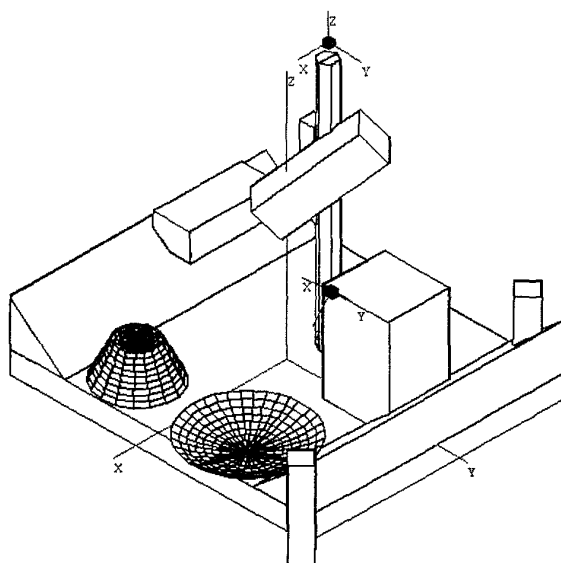


Figure 6. An array configuration.

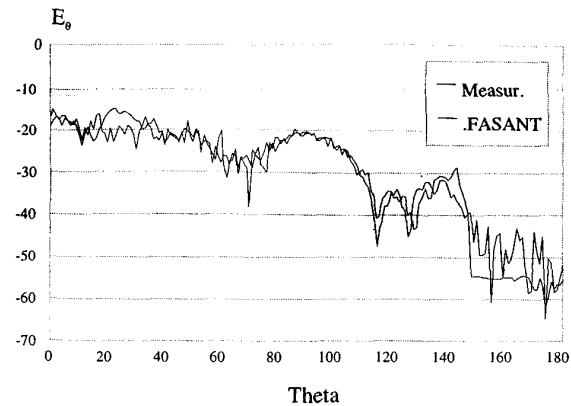


Figure 7. A comparison between the measured and computed radiation-pattern values: Cut  $\phi = 270^\circ$ ,  $E_\theta$  component.

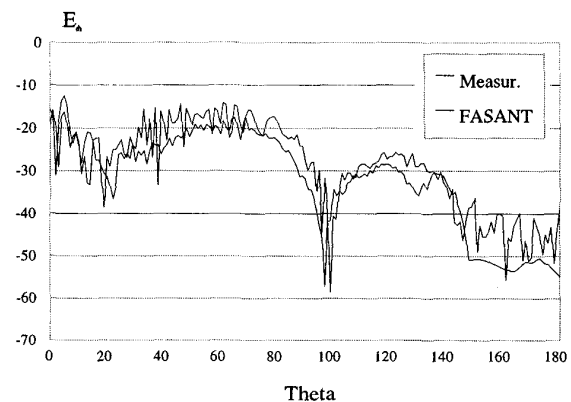


Figure 8. A comparison between the measured and computed radiation patterns:  $E_\phi$  component in the  $\phi = 270^\circ$  cut.

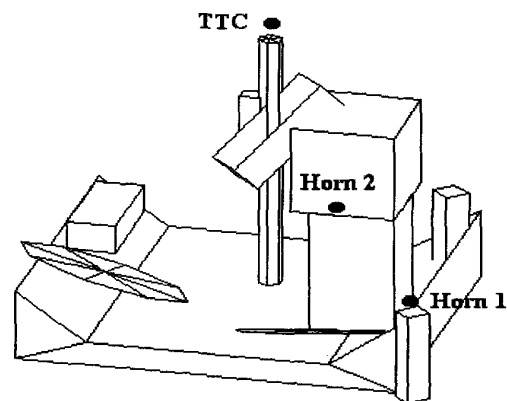


Figure 9. The geometry for the coupling cases.

The magnitude of the field for each of its components ( $E_\theta$ ,  $E_\phi$ ;  $E_{U_i}$ ,  $E_{U_d}$  for the far field;  $E_x$ ,  $E_y$ ,  $E_z$ , for the near zone) can be visualized individually. Also, the field due to any set of ray mechanisms can be represented.

## 5.2 Ray tracing

Ray tracing is visualized from any point of view. It is possible to visualize the rays of any set of coupling mechanisms. Figures 5a and 5b show an example of ray tracing in a ship [Editor's note: although not reproduced here, the various ray paths are shown in color]. This option is very useful for understanding the multiple ray mechanisms.

## 6. Validation

Far-field and coupling data for antennas on board the HISPASAT satellite are presented, to show the accuracy of *FASANT*. With these results, the computation of the field level at near-zone points is also accomplished, because *FASANT* computes the antenna coupling using the reaction theorem [5]. The latter involves the evaluation of the field over a given antenna-aperture location, due to incidence from a pre-specified direction. The results are compared with measurements made by INTA (the Spanish Aerospace Agency), using a mock-up of the HISPASAT satellite. This mock-up is a scale model, with the following dimensions: 1.43 m  $\times$  1.66 m in the box, with a height of 0.13 m in the middle, and 0.386 m along each lateral direction. The maximum height of the model (the mast) is 1.403 m.

Results for an array of two antennas, located in the satellite mockup of Figure 6, are presented. The coordinates of the first antenna, which is over the mast, are (-0.1859, 0.0496, 1.4753) meters. The other antenna is located at (0.1594, 0.4089, 0.6156) meters. Figures 7-8 show the  $\phi = 270^\circ$  cut for the  $\theta$  and  $\phi$  components of the radiation pattern.

### 6.1 Coupling validation

The model used for validation is shown in Figure 9. Five measurements were made, using three antennas: two horns and a TTC (see Figure 9). In each case, a pair of antennas was used in a transmit/receive configuration, as indicated in Table 1.

Table 2 presents the results, referring to all measurements at the indicated frequencies. Measurement configurations 1 and 2 were made in an anechoic chamber. Measurements for configurations 3 and 4 were carried out at a different EMC chamber. The object of performing these four measurements, for the coupling of each transmitter-receiver pair, was to obtain an idea of the errors due to echoes in the chamber walls.

Table 3 gives the corresponding coupling results for five configurations using *FASANT*. The first column gives errors as compared to each measurement.

**Table 1. The antennas used for each coupling test configuration.**

Configuration	T <sub>x</sub>	R <sub>x</sub>
1	Horn 1	Horn 2
2	TTC	Horn 1
3	TTC	Horn 2
4	Horn 2	Horn 1
5	TTC	Horn 1

**Table 2. The measurement results for each T<sub>x</sub>-R<sub>x</sub> configuration, in dB.**

Error! Bookmark not defined.Config uration	f(GHz)	(1)	(2)	(3)	(4)
1	8	-85.7	-85.0	-79.3	-76.5
1	12	-78.9	-80.0	-84.3	-80.1
2	8	-77.5	-77.1	-69.8	-68.5
3	8	-80.3	-80.4	-78.6	-75.1
3	12	-	-	-87.7	-82.1
4	8	-71.4	-71.8	-71.6	-70.1
5	8	-90.5	-91.2	-87.1	-80.6

**Table 3. *FASANT* calculations corresponding to the measurement cases in Table 2.**

Error! Bookmark not defined.Config uration	f(GHz)	Calculated	E(1)	E(2)	E(3)	E(4)
1	8	-71.2	14.5	13.8	8.1	5.3
1	12	-80.8	0.9	0.8	3.5	0.7
2	8	-79.4	1.9	2.3	9.6	10.9
3	8	-85.9	5.6	5.5	7.3	10.4
3	12	-88.2	-	-	0.5	6.1
4	8	-70.9	0.5	0.9	0.7	0.8
5	8	-89.4	1.1	1.8	2.3	8.8

## 7. Acknowledgements

This work has been supported in part by SAAB and CICYT (Project No. TIC: TIC:96-0653).

## 8. References

1. D. A. McNamara, C. W. I. Pistorius, J. A. G. Malherbe, *Introduction to the Uniform Theory of Diffraction*, Norwood, MA, Artech House, 1989.
2. M. F. Cátedra, J. Pérez, F. Saez de Adana, O. Gutierrez, "Efficient Ray-Tracing Techniques for Three-Dimensional Analyses of Propagation in Mobile Communications: Application to Picocell and Microcell Scenarios," *IEEE Antennas and Propagation Magazine*, 40, 2, April 1998, pp. 15-28.
3. G. Farin, *Curves and Surfaces for Computer Aided Geometric Design, Third Edition*, London, Academic Press, 1992.
4. C. A. Balanis, *Antenna Theory: Analysis and Design*, New York, John Wiley and Sons, 1982.
5. V. H. Rumsey, "The Reaction Concept in Electromagnetic Theory," *Physical Review (Series 2)*, 1954, pp. 1483-91. 